

Supporting Information

Contents

Figure S1. Pore size distribution of SiO_2 and SiO_2 - TiO_2 aerogel particles.

Figure S2. Pore size distribution of pure TiO_2 photoanode and typical aerogel photoanode.

Figure S3. SEM image of aerogel photoanode with high percentage of aerogel incorporated.

Figure S4. Typical J-V curves of DSC based on pure TiO_2 , SiO_2 aerogel and SiO_2 - TiO_2 hybrid aerogel-modified photoanodes.

Figure S5. Electrochemical impedance spectra of DSCs based on pure TiO_2 and aerogel photoanodes.

Figure S6. Open-circuit voltage decay (OCVD) curves of DSCs based on pure TiO_2 and aerogel photoanodes.

Figure S7. External quantum efficiency of DSCs based on pure TiO_2 and aerogel photoanodes.

Table S1. EIS parameters obtained by fitting the Nyquist plots with the equivalent circuit for DSCs based on pure TiO_2 and aerogel based photoanodes.

Figure S1. Pore size distribution of SiO₂ and SiO₂-TiO₂ aerogel particles obtained from N₂ adsorption-desorption measurement, illustrating the change of the pore size in aerogel with the deposition of TiO₂ nanoparticles deposited on SiO₂ template.

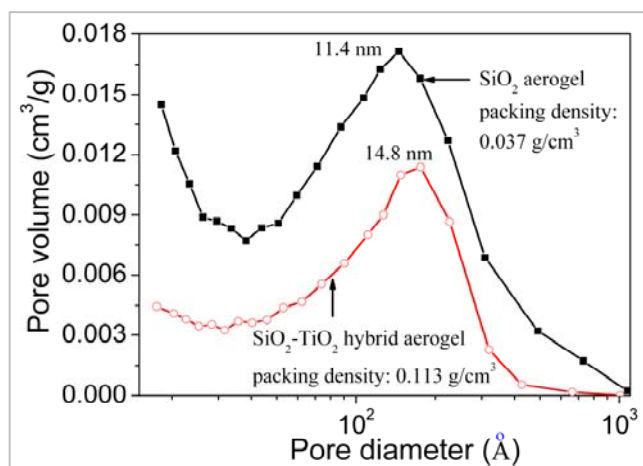


Figure S2. Pore size distribution of pure TiO₂ photoanode and SiO₂-TiO₂ aerogel photoanode obtained from N₂ adsorption-desorption measurement.

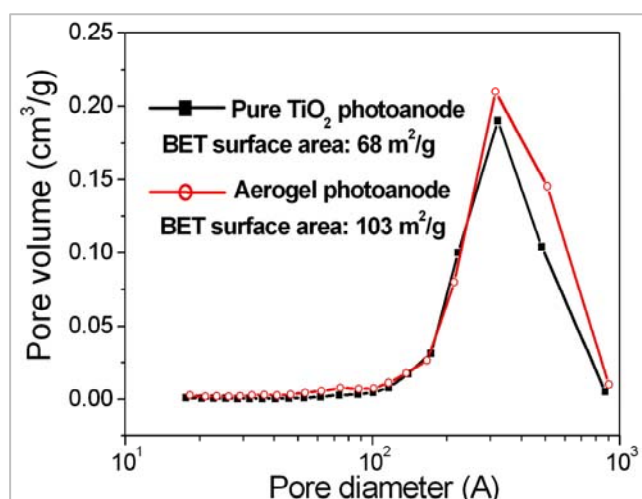


Figure S3. SEM image of aerogel based photoanode film with high percentage of $\text{SiO}_2\text{-TiO}_2$ aerogel incorporated in the slurry of hydrothermal TiO_2 nanoparticles (ATP value: 30%), illustrating that the large-size aerogel particles may induce large amount of cracks in the film and deteriorate the overall film quality.

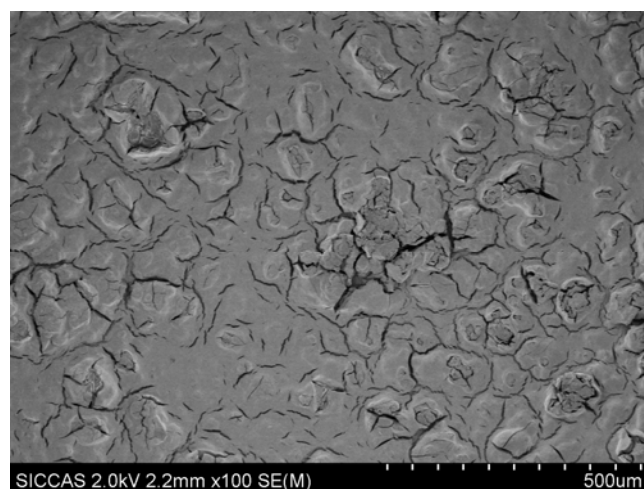


Figure S4. Typical J-V curves of DSC based on pure TiO_2 , SiO_2 aerogel and $\text{SiO}_2\text{-TiO}_2$ hybrid aerogel-modified photoanodes.

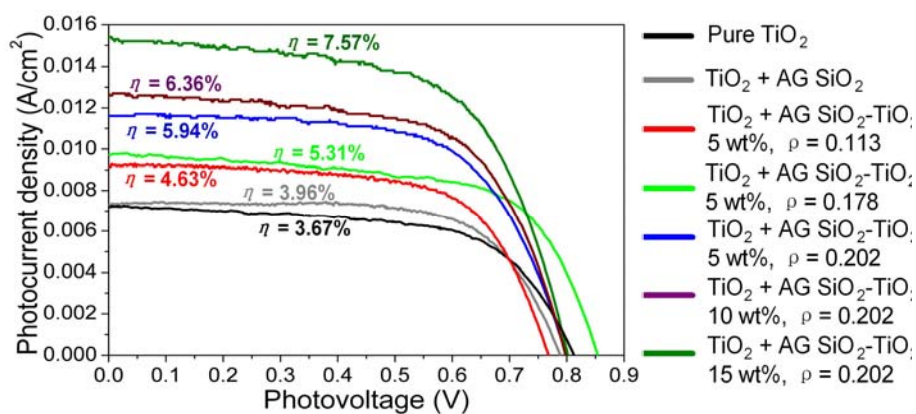


Figure S5. a) Electrochemical impedance spectra (left) of DSCs based on pure TiO_2 and aerogel based photoanodes, illustrating that the aerogel based cell has the similar recombination frequency with the pure TiO_2 cell. b) Equivalent circuit used for the calculation of EIS parameters.

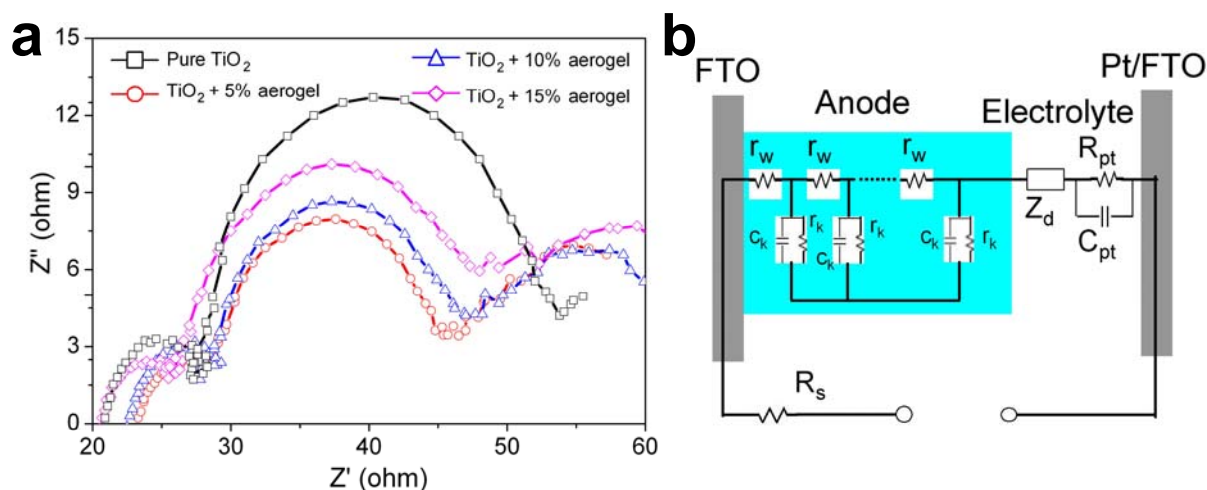


Figure S6. Open-circuit voltage decay (OCVD) curves of DSCs based on pure TiO_2 and aerogel based photoanodes, illustrating that aerogel photoanodes have much faster recombination between electron and the electrolyte than pure TiO_2 photoanode.

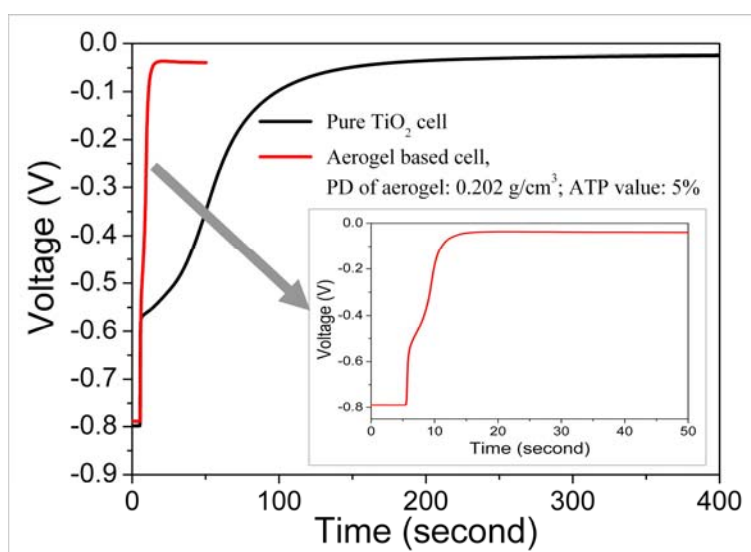


Figure S7. External quantum efficiency of DSCs based on pure TiO₂ and aerogel based photoanodes, illustrating that aerogel photoanodes have much higher light-harvesting capacity than pure TiO₂ photoanode.

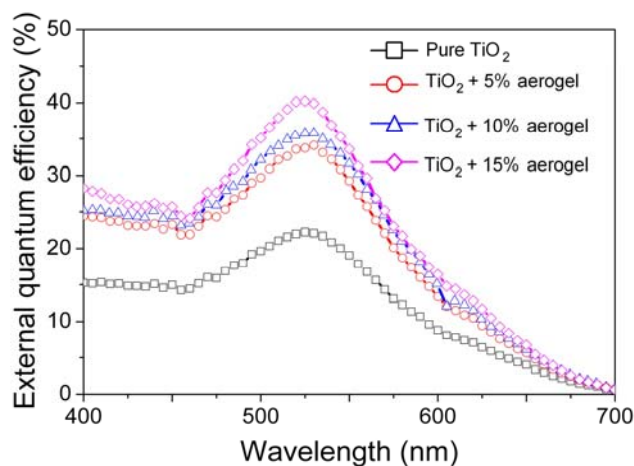


Table S1. EIS parameters obtained by fitting the Byquist plots with the equivalent circuit in Figure S5b for DSCs based on pure TiO₂ and aerogel based photoanodes.

Electrode	R _w (Ω)	R _k (Ω)	k _{eff} (s ⁻¹)	τ _{eff} (ms)	D _{eff} (cm ² /s × 10 ⁻⁴)
Pure TiO ₂	5.15	130.80	25.7	39	8.93
TiO ₂ + 5% aerogel ^a	4.10	78.89	25.7	39	5.46
TiO ₂ + 10% aerogel	4.35	84.46	25.7	39	5.30
TiO ₂ + 15% aerogel	4.78	111.30	21.23	47	5.98

[a] Packing density of SiO₂-TiO₂ hybrid aerogel: 0.202 g/cm³.